

International Conference on Space Optics—ICSO 2012

Ajaccio, Corse

9–12 October 2012

Edited by Bruno Cugny, Errico Armandillo, and Nikos Karafolas



BepiColombo fine sun sensor

Erik Boslooper

Nico van der Heiden

Daniël Naron

Ruud Schmits

et al.



BepiColombo Fine Sun Sensor

Erik Boslooper, Nico van der Heiden, Daniël Naron, Ruud Schmits, Jacob Jan van der Velde, Jorrit van Wakeren
TNO, P.O. Box 155, 2600 AD Delft, The Netherlands
erik.boslooper@tno.nl

Abstract - Design, development and verification of the passive Fine Sun Sensor (FSS) for the BepiColombo spacecraft is described. Major challenge in the design is to keep the detector at acceptable temperature levels while exposed to a solar flux intensity exceeding 10 times what is experienced in Earth orbit. A mesh type Heat Rejection Filter has been developed. The overall sensor design and its performance verification program is described.

Keywords: BepiColombo; Fine Sun Sensor; Heat Rejection Filter; quadrant detector; mesh filter

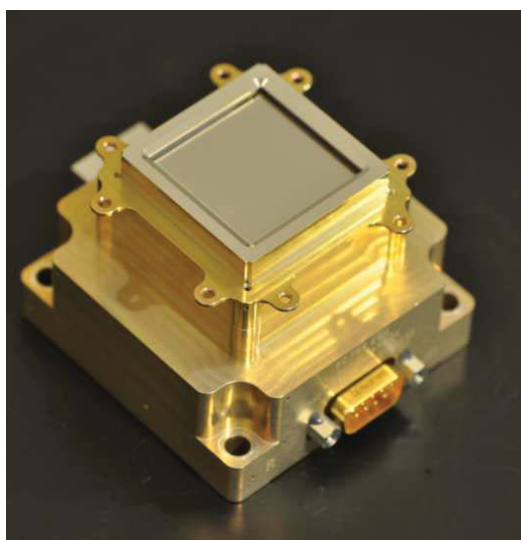


Figure-1. BepiColombo Fine Sun Sensor

1. INTRODUCTION

The BepiColombo mission to Mercury is an ESA corner stone mission in co-operation with the Japanese Space Agency JAXA. This paper describes the design, development and verification of the passive Fine Sun Sensor (FSS), which is part of the spacecraft (S/C) Attitude and Orbit Control System (AOCS). Measurement of the sun direction relative to the S/C constitutes the basis for the S/C survival mode featuring a safe thermal orientation. The sensor is based on a quadrant type detector as it was earlier used for other missions. As near Mercury the sensor will be exposed to solar fluxes exceeding

10 times those in Earth orbit, the main challenge is to keep the sensor within reasonable temperature limits. For this purpose a dedicated Heat Rejection Filter has been developed, which is put in front of the quadrant detector.

2. QUADRANT DETECTOR FSS OPERATING PRINCIPLE

The BepiColombo FSS is an analogue fine sun sensor, based on the use of a quadrant type detector: a chip with four active elements. This type of detector has been developed by OSI Electronics based on TNO specification and design. Meanwhile TNO, together with Moog Bradford Engineering-NL, has delivered sun sensors with this type of detector for the GAIA mission as well as for several commercial programs. To limit FSS development costs and risks, a detector of the same family was selected for use in the BepiColombo sun sensor.

The quadrant detector is a p-n junction silicon photodiode. Closely above the detector active surface, a square aperture mask is accurately positioned. Sunlight reaches the detector through the mask. The distribution of the incident sunlight across the four quadrants and the induced photocurrents, which are proportional to the illuminated quadrant areas, depend on the solar angle of incidence (Fig. 2). Thus, within the sensor Field of View (FoV), the solar aspect angle can be calculated in terms of two angles α and β , which define the rotation of the sensor around the X and Y axes respectively.

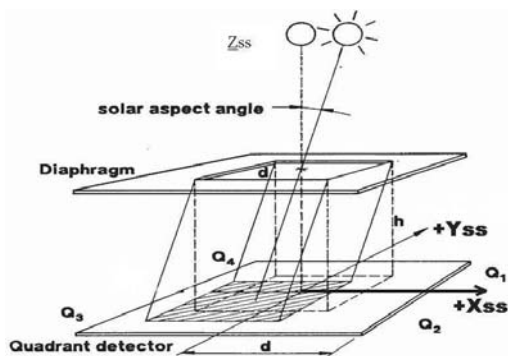


Figure-2. Quadrant sensor operation principle



Figure-3. FSS quadrant detector module for BepiColombo

The relation between the quadrant signals and the solar angles of incidence is given by the following simple formula (1) and (2).

$$S_A = \frac{Q_2 + Q_3 - Q_1 - Q_4}{Q_1 + Q_2 + Q_3 + Q_4} = \frac{\tan(\alpha)}{\tan(\alpha_{MAX})} \quad (1)$$

$$S_B = \frac{Q_1 + Q_2 - Q_3 - Q_4}{Q_1 + Q_2 + Q_3 + Q_4} = \frac{\tan(\beta)}{\tan(\beta_{MAX})} \quad (2)$$

The α_{MAX} and β_{MAX} are the maximum solar aspects angles as defined by the quadrant detector geometry and are defined by:

$$\alpha_{MAX} = \beta_{MAX} = \frac{d}{2h} \quad (3)$$

where d is the (square) aperture diameter and h the distance between the aperture mask and the detector active surface.

The sensor FoV depends on the distance between the aperture mask and the detector sensor active area as well as on the size of the aperture. No lenses or other optically active elements are involved. The TNO BepiColombo FSS just delivers analogue currents to the Remote Interface Unit (RIU), which converts these into voltages and performs 16-bit digitization. The algorithm to calculate the respective sun angles of incidence from the quadrant signals, runs in the spacecraft on-board computer.

The FSS performance relies on an unambiguous relationship between detector output signal and solar angle of incidence, via the so-called S-value as calculated from the quadrant measurement currents using (1) and (2). The quadrant currents as function of the solar angle of incidence are shown in Fig. 4. The solid line in Fig. 5 is the corresponding S-value. Further details related to Fig. 4 and Fig. 5 will be explained in following.

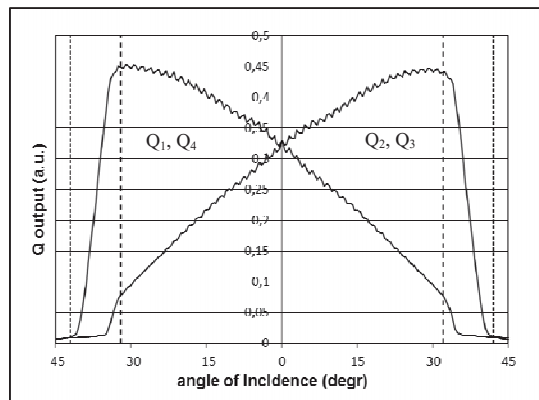


Figure-4. Quadrant signal as function of angle of incidence. The ripple on the signal is caused by the mesh filter. Vertical lines designate $\pm 32^\circ$ and $\pm 42^\circ$ respectively.

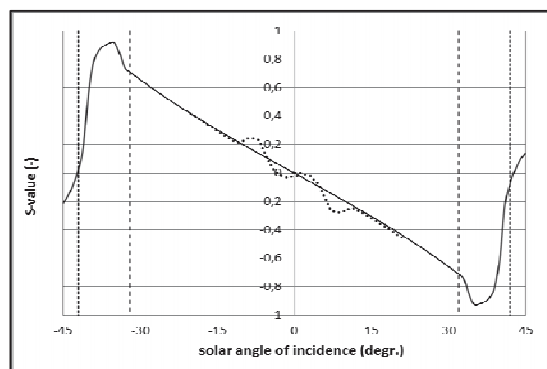


Figure-5. S-value as function of the angle of incidence as calculated from the quadrant signals. The solid line represents the mesh filter, the dotted line represents an optical bandpass filter (see section 4).

3. THE BEPICOLOMBO FSS

The FSS requires a free view to the sun. Any non direct sunlight reaching the FSS detector, negatively impacts the accuracy. Thus reflections or shading from spacecraft element like solar panels, antenna's etc. shall be avoided. To limit this so-called unobstructed FoV, a top baffle is implemented at some height above the detector module to create a cut-off at 42° , i.e. sunlight with an angle of incidence $> 42^\circ$ shall not reach the detector. This top baffle determines the overall size of the FSS and its optical aperture of approximately 30×30 mm. For a mission to Mercury like BepiColombo, where the sensor will be exposed to solar fluxes exceeding 10 times those seen in Earth orbit, the main challenge is to ensure reasonable temperatures. To this end, TNO has developed a dedicated Heat Rejection Filter, which is positioned on the top baffle and closing the complete optical aperture. To allow for some mechanical fixation, the filter substrate size is 37×37 mm and the FSS top area is 40×40 mm. Once the spacecraft thermal blankets are installed, this 40×40 mm top area is the only part of the FSS which is visible, i.e. exposed to the sun.

4. DD&V OF THE HEAT REJECTION FILTER

A. Requirements

To prevent overheating of the sensor, the main function of the Heat Rejection Filter is to reflect the majority of the incident solar radiation. On the other hand, to ensure adequate detector currents, some light shall be transmitted. Finally, the filter shall not degrade in the BC space environment. Possible design solutions considered are:

- a narrow bandpass optical reflection filter
- mesh filter

The required unambiguous relationship between detector output signal and solar angle of incidence (section 2) cannot be obtained with a narrow bandpass filter.

As can be understood from Fig. 6, unlike an ideal bandpass filter, any realistic bandpass filter will reflect part of the incident light via the edges, the wavelength band in which the transmission “switches” between minimum and maximum, which results in light initially reflected from the detector, being back-reflected towards the detector via the HRF. The resulting ghosts result in a non-unambiguous relationship between detector output signal and solar angle of incidence (dotted line in Fig. 5). This leads to the requirement that the detector facing surface of the HRF shall have a low reflectivity (at least in the relevant bandpass).

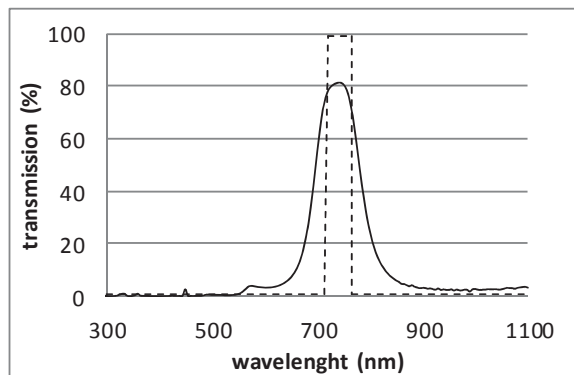


Figure-6. Ideal versus realistic optical bandpass filter characteristic.

B. Mesh filter design

The inherent problem with a non-ideal bandpass filter has been solved by using a mesh type filter: a high reflective coating with a regular pattern of small holes to transmit the light. A dedicated multilayer coating has been designed, which is highly reflective at the space facing side (Aluminum) and black at the detector facing side, thus resulting in negligible back-reflections onto the detector (solid line in Fig 5). As a random hole pattern would result in speckle like structures, a regular grid has been selected for the mesh filter. For production reasons square instead of circular openings have been selected. To investigate the inherent diffraction effects, the optical performance of the mesh filter has been modeled in a two-step approach:

1. Diffraction analysis, depending on the width of the openings, confirms applicability of the far field approximation and yields the relative intensity of the different diffraction orders.
2. Filter level optical performance analysis, showing FoV cut-off behaviour and light distribution on the detector. This analysis depends on the spacing between the openings.

Due to higher order effects, there will be non-zero sensitivity for light from outside the unobstructed FoV, i.e. with angles of incidence $> 42^\circ$. The FoV cut-off behavior depends on the spacing between the openings. This parameter has been optimized to ensure a light falling through a reasonable number of opening (for all quadrants) in the complete FoV and relatively sharp cut-off between the 32° edge of the nominal FoV and the 42° blinding angle (Fig. 4). The size of the openings has been selected to result in a nominal filter transmission about 16%, yielding still acceptable detector currents just after launch (with only 1 Solar Constant intensity).

C. Development

Sapphire has been selected as HRF substrate for its relatively good thermal conductivity. However, as the sapphire substrates are difficult to process and the damage of the coating shall be prevented, the perforated coating has to be applied on the substrates in their final square dimensions. As illustrated in Fig. 7, the mesh filter is produced according to a lithographic process, encompassing the following main steps:

1. application of the photoresist by spin-coating
2. lithographic exposure
3. resist development, resulting in a “negative” mesh filter
4. application of multilayer coating
5. lift-off, i.e. remove the remaining resist layer

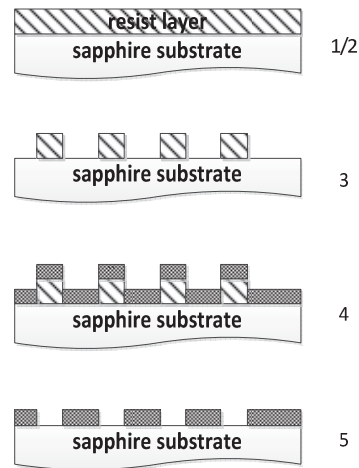


Figure-7. Schematic of the mesh filter production steps, the numbers correspond with the numbers in the text.



Figure-8. Special tooling to enable spin-coating of the square sapphire substrates.

In the last step the remaining resist is removed, along with the coating applied on top. This results in the mesh coating applied on the substrate. As the standard lithographic tooling is designed for the processing of circular Si-wafers, dedicated tooling had to be designed and manufactured to enable the processing of the square sapphire substrates during spin-coating, lithographic exposure, resist development, coating application and lift-off. The filter manufacturing has been performed in ultra-clean environment in the TNO cleanroom facilities.

D. Verification

The mesh filters have been subjected to an extensive test program, including the standard coating tests: adhesion, solubility and humidity. The specific test program for BepiColombo involved optical properties testing at elevated temperature (125 °C), proton and electron radiation testing, thermal cycling and (V)UV testing. The filter was demonstrated to be able to withstand the harsh BepiColombo environment. The (V)UV test however showed a limited degradation of the filter optical properties which can be completely attributed to contamination in combination with (V)UV illumination. It turns out that under the influence of high energetic short wave Vacuum UV (< 200 nm) polymerization of contaminants occurs. However, considering the FSS worst case expected contamination level on the S/C, the filter absorption increase is still well within the acceptable range. The final mesh filter is shown in Fig. 9.

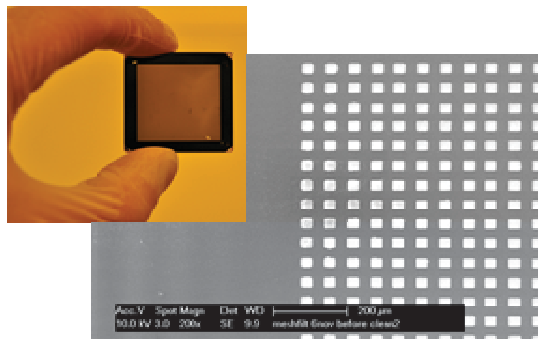


Figure-9. Resulting mesh filter and detail.

5. FSS UNIT LEVEL VERIFICATION

A. Performance testing and calibration

During the unit level performance test, the sensor is installed on a two-axes rotary unit in the TNO sun simulator test bench (Fig. 10). The sun simulator produces a beam with an intensity of approximately 1 solar constant. The beam divergence ~1.5 degree, which is close to the apparent sun diameter seen at Mercury in perihelion. As the quadrant photodiodes in the detector behave strictly linear with an increase in light intensity, testing can be done at one tenth of the intensity near Mercury.

The FSS unit will be installed and adjusted in the test set-up by means of auto-collimation measurements on the alignment cube of the FSS (just visible at the side opposite to the connector in Fig. 1). During assembly it is ensured that the alignment cube axes and the sensor electro optical axes are aligned with an accuracy of <math><0.03^\circ</math>. After sensor alignment in the solar simulator, a scan is made through the main axes of the FoV (alpha and beta). Thus the sensor FoV and accuracy are verified.

B. Environmental testing

On unit level, the FSS was subjected to a complete environmental qualification test program, including vibration, shock, thermal and EMC testing. The complete thermal test program consisted of 3 different parts.

Performance testing in thermal vacuum, including 8 thermal cycles to qualification level (-45 / +115 °C). In this test, the sensor is mounted on a single axis rotary unit mounted inside a thermal vacuum facility with a window through which the sensor is illuminated by the same sun simulator as in the (ambient) performance test. A temperature coefficient, for use in the on-board processing, is determined from the difference in unit response at several different temperature levels, covering the in-orbit experienced temperature range.

A high intensity solar test is performed at a facility of the university of Bern. In this test, the unit was mounted thermally representative to S/C mounting conditions to the extent possible and exposed to a 5.7 SC solar simulator. This test has been used for Thermal Mathematical Model correlation.

Thermal cycling test in dry nitrogen. In this test the passive unit has been subjected to 1950 thermal cycles (-24 / + 101 °C), simulating the eclipses the FSS will be subjected to in Mercury orbit.

C. Calibration testing of flight FSS

After completion of the environmental (acceptance) test program, an on-ground calibration is performed on each flight unit. Differences between the sensor measured S-value (from quadrant signals) and the nominal, theoretically expected S-value (from rotation table settings) are determined for many different angular positions in a pre-determined grid covering the complete FoV. These differences are processed for storage in on-board look-up tables. The program is concluded with a so-called random scan consisting of 1000 points randomly distributed over the complete FoV. Using the previously

determined in-flight calibration tables, the residual error is calculated for each of the 1000 points.

The on-board calibration tables consist of 8-bit numbers covering the complete FoV via 33 x 33 points. As separate tables exist for the α and β directions, the total memory load is 2.2 kByte. During on-board processing, the measured S-value is corrected by 2 dimensional linear interpolation.

Excluding the electronics error contribution, after calibration, the FSS achievable accuracy is better than 0.36° . Unlike the electronics induced error, this error is independent from the signal level, i.e. solar distance.



Figure-10. Test set-up for performance testing and calibration with solar simulator and FSS mounted on 2-axis rotation table.

6. OPERATIONAL ASPECTS

In the on-board processing, the sensor solar incidence angle is calculated in terms of α and β from the ratio of the measured quadrant currents using (1) and (2). The first step in the on-board processing is to establish whether the sun is actually in the nominal FoV. This is done by comparing the signal level with actual value of the so-called sun presence threshold parameter. The function of this parameters is twofold:

1. to distinguish between sun and planetary albedo and,
2. to ensure a unambiguous relationship between the S-value and the solar incidence.

By design, the quadrant sensor concept is sensitive to albedo. The only possible distinction between the sun and planetary albedo is based on the signal level. Ensuring proper sun presence threshold values, sufficiently large albedo safety margins can be achieved during the planetary flyby.

The sensor gives a current output, and thus an S-value can be calculated, up to at least 42° angle of incidence (Fig. 4). Although S-values calculated for angles of incidence $> 32^\circ$ are not unambiguous anymore, they do not overlap those of the $\pm 32^\circ$ performance range up to about 40° (Fig. 5). Thus, when the calculated S-value is in this range, the output of the algorithm will be that the sun is not in the sun sensor $32^\circ \times 32^\circ$ FoV. For angles of incidence $> 40^\circ$, the current values are below the sun presence threshold and no S-value is calculated at all.

Considering the required margins and overlap, up to about a factor 3 in solar intensity variation can be coped with via a single sun presence threshold value. During cruise phase to Mercury, there is a strong variation in solar intensity, with a factor 14 between the minimum and maximum value. Thus, in-flight, multiple updates of the sun-presence threshold parameter are foreseen. Considering also the required distinction between worst case planetary albedo signal during flyby and sun induced signal, fixed solar distance ranges have been defined in which a single threshold value can be used. The actual values are unit specific and will be determined during on-ground calibration.

ACKNOWLEDGEMENT

The work described has been performed under contract with Astrium GmbH. The authors wish to thank the colleagues in Friedrichshafen for pleasant cooperation.